J. CHEM. SOC. FARADAY TRANS., 1994, 90(7), 1015–1022

# Adsorption and Decomposition of Methanol on $TiO_2$, $SrTiO_3$ and SrO

**Nina Aas, Thomas J. Pringle and Michael Bowker†**
*Leverhulme Centre for Innovative Catalysis and Surface Science Research Centre, University of Liverpool, P.O. Box 147, Liverpool UK L69 3BX*

The adsorptive and reactive behaviour of $TiO_2$, $SrTiO_3$ and SrO towards methanol have been investigated using temperature-programmed desorption and XPS. $TiO_2$ was found to be reduced during the adsorption/desorption process and showed predominantly $CH_4$ formation at low coverages. At higher coverages, alternative paths led also to the desorption of $CH_3OH$ and HCHO though $CH_4$ was the main product desorbed at *ca.* 500 K. The product pattern indicates that a methoxy is the major surface intermediate. CO and $H_2$ were evolved at *ca.* 600 K, possibly from the decomposition of a formate species, while $H_2O$ was desorbed between 300 and 700 K. On SrO the coincident evolution of CO and $H_2$ at 580 K, with $H_2O$ and $CO_2$ being minor products, indicated a formate intermediate as the dominant one on this surface. The product pattern on $SrTiO_3$ resembled that on $TiO_2$, although the main product in this case was $CH_3OH$, with $CH_4$ being produced in much smaller quantities and only at much higher temperature than on $TiO_2$ (620 K). The source of these differences is discussed in terms of the defect chemistry of the surfaces involved.

Because of their thermal stability and their easy preparation into high-surface-area materials, oxides have a long history of being used as supports for catalysts.[1] However, they can also operate as catalysts themselves. Kung[2] has summarised some of the reactions catalysed by transition-metal oxides. These range from dehydrogenations, selective oxidations and reductions, to the water-gas shift reaction. In spite of their inherent advantages mentioned above, oxides are complex materials, a fact which is also pointed out by Kung.[2] They are generally polycrystalline in nature, which means that the surface is far from homogeneous. Furthermore, their surfaces contain defects, can be enriched or depleted in one element and can vary in chemical state (*e.g.* hydroxylation). These and further factors listed by Kung underline the importance of well controlled preparation conditions and the subsequent careful characterisation which is essential for understanding the surface chemistry and hence the reactivity of oxides.

The interaction of methanol with oxide surfaces represents a good test of surface chemistry. It is as part of a broader programme aimed at extending the knowledge of the reactivities of oxide surfaces that the interaction of methanol with $TiO_2$ (rutile), $SrTiO_3$ and SrO has here been investigated. $TiO_2$ in its various crystal modifications is widely used as a catalyst support and is probably most associated with the SMSI effect.[3,4] It has also been employed in photoassisted reactions,[5] as have SrO and $SrTiO_3$. The latter has been investigated in the photocatalytic water splitting reaction under zero applied potential in its pure form[6] and in combination with NiO.[7] SrO has found little use in catalysis,[8,9] but it has been investigated in terms of its acid–base properties[10] and its formation of different surface states upon heating.[11] More recently, there has been some interest in doping $La_2O_3$ used in the oxidative coupling of methane with Sr,[12,13] and the alkaline-earth-metal oxides and carbonates have been re-examined with XPS because of their potential usefulness in superconducting materials.[14]

$SrTiO_3$ is a mixed oxide. It can be prepared by mixing $SrCO_3$ and $TiO_2$ in a 1 : 1 ratio and heating at 1273 K for a prolonged period.[15] In terms of crystallographic structure it belongs to the class of perovskites, although its basic building blocks, which are $TiO_6$ octahedra, are the same as those of $TiO_2$ (rutile). In the 1970s, the photodecomposition of $H_2O$ under conditions of band-gap illumination on both $SrTiO_3$ as well as on $TiO_2$ inspired a lot of work relating these observations to the structural and electronic properties of the oxides under both oxidising and reducing conditions. These studies were generally carried out on single crystals and established the link between the oxide reactivity and the existence of surface defects.[16–22] For instance, in the case of $SrTiO_3(111)$, the stoichiometric surface showed photoelectron peaks indicative of $Sr^{2+}$, $Ti^{4+}$ and $O^{2-}$ including some residual hydroxy groups. The surface was inert to $O_2$ and $H_2$ exposure even under illumination. If this oxide was bombarded with argon ions, oxygen ions were preferentially removed, which led to an increase in the observed Sr : O ratio and to the appearance of $Ti^{3+}$ in the spectrum. The surface thus produced was very reactive to $O_2$ resulting in reoxidation of $Ti^{4+}$.[16]

$TiO_2$ single-crystal studies have shown a range of similarities with $SrTiO_3$.[19–22] Lo *et al.* found that oxygen deficiency could be introduced by prolonged heat treatment at 1400 K[19,20] as well as by argon-ion bombardment. On $TiO_2(100)$, this led to a new surface structure as was seen in the change of the LEED pattern and in the appearance of $Ti^{3+}$ in the XPS spectrum. Both Lo *et al.*[20] and Heinrich *et al.*[21] observed an enhanced reactivity of the reduced surfaces towards adsorbates containing oxygen. The different nature of the defects introduced by either heat treatment or argon-ion bombardment has been discussed by Göpel *et al.*[22]

All these studies have in common that they are mainly concerned with the adsorption of either $H_2$, $O_2$ and $H_2O$, that is adsorbates with direct relevance to water splitting. The overall conclusion from these studies is that the reduced surfaces tend to adsorb $O_2$ and $H_2O$ dissociatively and become more oxidised while the oxidised surfaces tend to adsorb these gases molecularly. More recent work on $TiO_2$ single crystals has concentrated on determining point defects[23] and on the adsorption of other small molecules like methanol,[24,25] formic acid[25] and ammonia.[26] These studies utilise the control over the surface stoichiometry that is achieved on single crystals and attempt to correlate results from adsorption experiments on these with similar results from oxide powders. We have here adopted a different approach. By using

---

† Present address: Department of Chemistry, University of Reading, Whiteknights Park, Reading, UK RG6 2AD.

methanol adsorption as a test reaction it is aimed to probe the surface of three related oxides and especially to establish how the mixed oxide surface is composed.

## Experimental

The methanol decomposition experiments were carried out in a small vacuum chamber which was equipped with a VG Monitorr quadrupole mass spectrometer operated by an Opus PC5 computer. The working background pressure was $5 \times 10^{-7}$ Torr.

The samples were mounted in a small silica tube which could be resistively heated *via* a Pt/Rh wire wound around it. A chromel–alumel thermocouple was inserted into the oxide powder to obtain accurate temperature measurements. The heating was carried out in a constant-current mode which meant that the heating rate varied over the range 300–800 K. In the range of interest it was 3 K $s^{-1}$, and it varied little over the region of a peak.

$TiO_2$, $SrTiO_3$ and $SrCO_3$ were supplied by Johnson Matthey and were of 99% purity. SrO was prepared from $SrCO_3$ by calcining it at 1200 K in air for 1.5 h and crushing it before it was inserted into the vacuum chamber where it was further calcined at 973 K for 1 h. Methanol of 99.5% purity was supplied by BDH. It was further purified by cycles of freeze–pump thawing.

Prior to use each oxide was heated in $1 \times 10^{-4}$ Torr oxygen for 1 h at 773 K to remove any carbon contamination, and it was then briefly annealed at 773 K *in vacuo* before the adsorption experiments took place.

XP spectra of the three oxides were generated using a VG ESCA 3 mk I instrument. The oxides were pressed into discs and mounted on a Cu sample holder. They underwent the same heat treatment at 773 K *in vacuo* as described above before the spectra were recorded. The working background pressure was $5 \times 10^{-9}$ Torr, and the spectra were obtained with Al-K$\alpha$ radiation of 160 W using a pass energy of 50 eV and an angle of electron escape of 45°.

## Results

### XPS Investigation of the Oxides

Fig. 1 shows the Ti 2p, O 1s and Sr 3p/C 1s regions of the spectra obtained from the three oxides. The relevant peak positions from these are summarised in Table 1, and they are quoted relative to C 1s = 285.0 eV. The Ti 2p region from both $TiO_2$ and $SrTiO_3$ consists of two single peaks in the approximate ratio of Ti $2p_{3/2}$ : Ti $2p_{1/2}$ = 2 : 1. For $TiO_2$, the separation of the two peaks is 5.7 eV and the FWHM of Ti $2p_{3/2}$ is 1.9 eV. The values for Ti in $SrTiO_3$ are identical, underlining the structural and chemical similarity of Ti in the two oxides. A comparison of the Ti $2p_{3/2}$ peak position with literature values indicates that it is in the oxidation state 4+. Carley *et al.*[27] found the most intense $Ti^{4+}$ peak in oxidised

**Table 1** XPS peak positions (binding energy in eV) of the most intense peaks in $TiO_2$, $SrTiO_3$, SrO and $SrCO_3$

| | Ti $2p_{3/2}$ | O 1s | Sr $3p_{3/2}$ | C 1s[a] |
|---|---|---|---|---|
| $TiO_2$ | 458.7 | 530.0 | | |
| $SrTiO_3$ | 458.4 | 529.7 | 268.6 | |
| SrO | | 531.5 | 269.2 | 289.7 |
| $SrCO_3$ | | 531.4 | 269.1 | 289.7 |
| $SrCO_3$[b] | | 531.5 | 269.0 | 289.5 |
| SrO[b] | | 528.2 | 268.1 | |

[a] C 1s peak other than the normal carbon reference at 285.0 eV. [b] Values quoted from ref. 14.

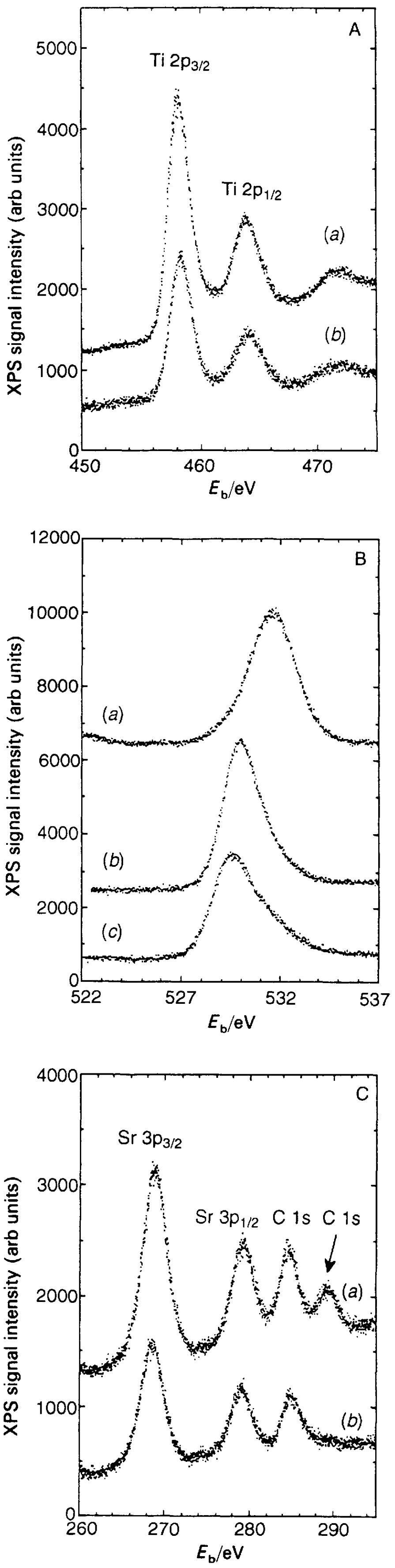

**Fig. 1** A, XP spectra showing the Ti 2p regions of (*a*) $TiO_2$ and (*b*) $SrTiO_3$. B, XP spectra showing the O 1s regions of (*a*) SrO, (*b*) $TiO_2$ and (*c*) $SrTiO_3$. C, XP spectra showing the Sr 3p/C 1s regions of (*a*) SrO and (*b*) $SrTiO_3$.

Ti foil at 459.0 eV, and the two Ti 2p peaks were separated by 6.0 eV. The argon-ion bombardment of their oxide film led to the appearance of suboxides with $Ti^{3+}$ at 457.5 eV and $Ti^{2+}$ at 455.3 eV, that is, they were well separated from the $Ti^{4+}$ peak. Sayers and Armstrong[28] who investigated a whole range of different titanium oxide powders and electrodes with XPS observed similar differences between Ti in different oxidation states as quoted above. They concluded that $Ti^{4+}$ in $TiO_2$ is very stable unless the compound is subjected to severe ion bombardment. Their work also included $SrTiO_3$ which in terms of Ti 2p peak positions, peak separation and FWHM was found to be identical to $TiO_2$.

The O 1s region shown in Fig. 1B confirms the similarity between the two oxides. The peak positions are identical within the limits of detectability, and in both cases the signal originates from more than one peak. Assuming the presence of two peaks of Gaussian shape, a peak fit for $TiO_2$ yields the main peak at 529.9 eV (FWHM 2.1 eV) and a second smaller peak at 531.8 eV (FWHM 2.4 eV) with an area ratio of these two peaks of 1 : 0.3. For $SrTiO_3$, the equivalent peak positions are 529.5 eV (FWHM 2.1 eV) and 531.6 eV (FWHM 2.4 eV), and the area ratio is 1 : 0.6. With reference to the literature quoted above these peak positions are indicative to oxide and hydroxide, respectively. It is concluded that in spite of the heat treatment *in vacuo* the surfaces of both oxides are extensively hydroxylated.

Fig. 1B further shows that the O 1s peak of SrO differs significantly from those of the other two oxides. Its position is at higher binding energies and its peak shape is asymmetrical with a tail to lower binding energies.

Fig. 1C shows the combined Sr 3p/C 1s regions of $SrTiO_3$ and SrO. Besides the Sr peaks which are located at binding energies typical of $Sr^{2+}$ [14,28] and which are identical in both oxides the main feature here is the additional peak at 289.7 eV in SrO (indicated by the arrow). By comparison with the literature[14] and with the spectrum of the starting material $SrCO_3$ from which SrO had been made this peak was identified as carbon in carbonate. The spectrum of $SrCO_3$ has not been included but the relevant peak positions are listed in Table 1, as are the literature values for $SrCO_3$ and SrO. On this basis, the O 1s region of SrO must be interpreted as being dominated by oxygen from carbonate. A peak fit of this region yielded the best results when assuming that it consisted of three Gaussian peaks. The first peak is located at 528.7 eV (FWHM 2.0 eV) and is attributed to oxide, the second at 530.7 eV (FWHM 2.0 eV) and identified as hydroxide, and the last one at 531.8 eV (FWHM 2.1 eV) which is typical of carbonate. The fitted peak area ratio is 1 : 5.5 : 7.6.

The presence of a mixture of oxygen-containing species on the surface of SrO is further confirmed by estimating the surface composition of the materials. Table 2 lists the atomic ratios of the main components in the three oxides. These were calculated according to Penn[29] using the XPS peak areas, the photoionisation cross-sections tabulated by Scofield,[30] the detection efficiency taken as $E^{-1}$ ($E$ being the kinetic energy of the photoelectron involved) and the mean free path of the photoelectrons based on Penn's formula. The ratios confirm that SrO is not pure oxide, that $TiO_2$ is essentially stoichiometric and that $SrTiO_3$ may be slightly deficient in Ti or enriched in Sr and O in the selvedge region.

**Table 2** Atomic ratios of the main components in the three oxides and in the carbonate which were derived according to ref. 29

| | Ti/O | Sr/O | Ti/Sr | Sr/C[a] | C[a]/O |
|---|---|---|---|---|---|
| $TiO_2$ | 0.58 | | | | |
| $SrTiO_3$ | 0.23 | 0.30 | 0.78 | | |
| SrO | | 0.40 | | 2.50 | 0.16 |
| $SrCO_3$ | | 0.38 | | 1.22 | 0.31 |

[a] C 1s peak area of carbon in carbonate, located at 289.7 eV.

## Thermal Desorption of Methanol adsorbed on $TiO_2$

The product distribution following the highest exposure of 3.0 Torr s is shown in Fig. 2A. The main products are CO, $CH_4$, $CH_3OH$ and $H_2$, with $H_2O$, HCHO and $(CH_3)_2O$ produced in smaller quantities. $CO_2$ was seen to be desorbed only at the higher temperature of 580 K and it was too small to be seen on this scale of the figure. The evolution of these species as a function of exposure is illustrated in Fig. 2B–G. The exposures used here were 0.12, 0.24 and 0.5 Torr s. Following the first exposure $CH_4$ is the major product being desorbed over a wide range of temperature, but with main peaks at *ca.* 460 K and *ca.* 650 K; small amounts of $CH_3OH$ and HCHO are also seen. The increase in exposure leads to an increase in the amount of $CH_4$ desorbed and to a decrease in the desorption temperature of the high-temperature state. The $CH_4$ evolution is now accompanied by CO, $CH_3OH$, HCHO, $H_2O$ and $H_2$. The intensity of all these desorption peaks increases with further exposure, the two stages of desorption being observed for $CH_4$, $CH_3OH$ and HCHO while CO and $H_2$ are only evolved in a single-temperature state. After dosing 3.0 Torr s of $CH_3OH$ the two desorption states are merged together to yield one broad peak. The $H_2O$ evolution occurs over the temperature range 350–700 K, and $CH_3OH$ is desorbed at around 415 K, slightly lower than $CH_4$, while HCHO is mainly evolved between 400 and 600 K. $(CH_3)_2O$ is only observed following the highest exposure and it is desorbed at 440 K.

At this stage, repeated adsorptions and desorptions did not change the surface, that is, the desorption spectra were identical for identical doses. However, at the end of these experiments the oxide was heated in oxygen (0.05 Torr for 15 min at 773 K) and then exposed to methanol. Now evolutions of $CO_2$ and $H_2O$ were seen below 373 K, the desorptions of $CH_3OH$ and HCHO were very much increased and the desorption of $CH_4$ decreased by around 50%. Repeated exposures of methanol followed by thermal desorption restored the original intensities.

## Thermal Desorption of Methanol adsorbed on SrO

The product distribution following an exposure of 0.15 Torr s of methanol is shown in Fig. 3. At this low dose the spectrum is dominated by the coincident evolution of CO and $H_2$ at 580 K. At higher exposures only the CO and $H_2$ desorptions continue to increase. The evolution of these as a function of exposure have therefore not been included. At the same temperature of the CO and $H_2$ desorptions there are also smaller amounts of $CO_2$, $H_2O$, HCHO and $(CH_3)_2O$. HCHO and $(CH_3)_2O$ were too small to be included in the figure. $CH_3OH$ is evolved at 405 and 470 K and is of low intensity compared with CO and $H_2$.

## Thermal Desorption of Methanol adsorbed on $SrTiO_3$

The product distribution is shown in Fig. 4A, and the dose dependence of the fragments is illustrated in Fig. 4B–E. The spectrum is dominated by the evolution of $CH_3OH$ around 440 K with $H_2$, $H_2O$ and $CH_4$ being lesser products. Coincident with $CH_4$ there are also traces of HCHO, CO, $CO_2$ and $H_2$ which are too small to be seen on this scale. $(CH_3)_2O$ evolution is not observed at all. From Fig. 4E it is seen that $CH_4$ is the main product following the lowest exposure. Although this resembles the behaviour of $CH_3OH$ on $TiO_2$

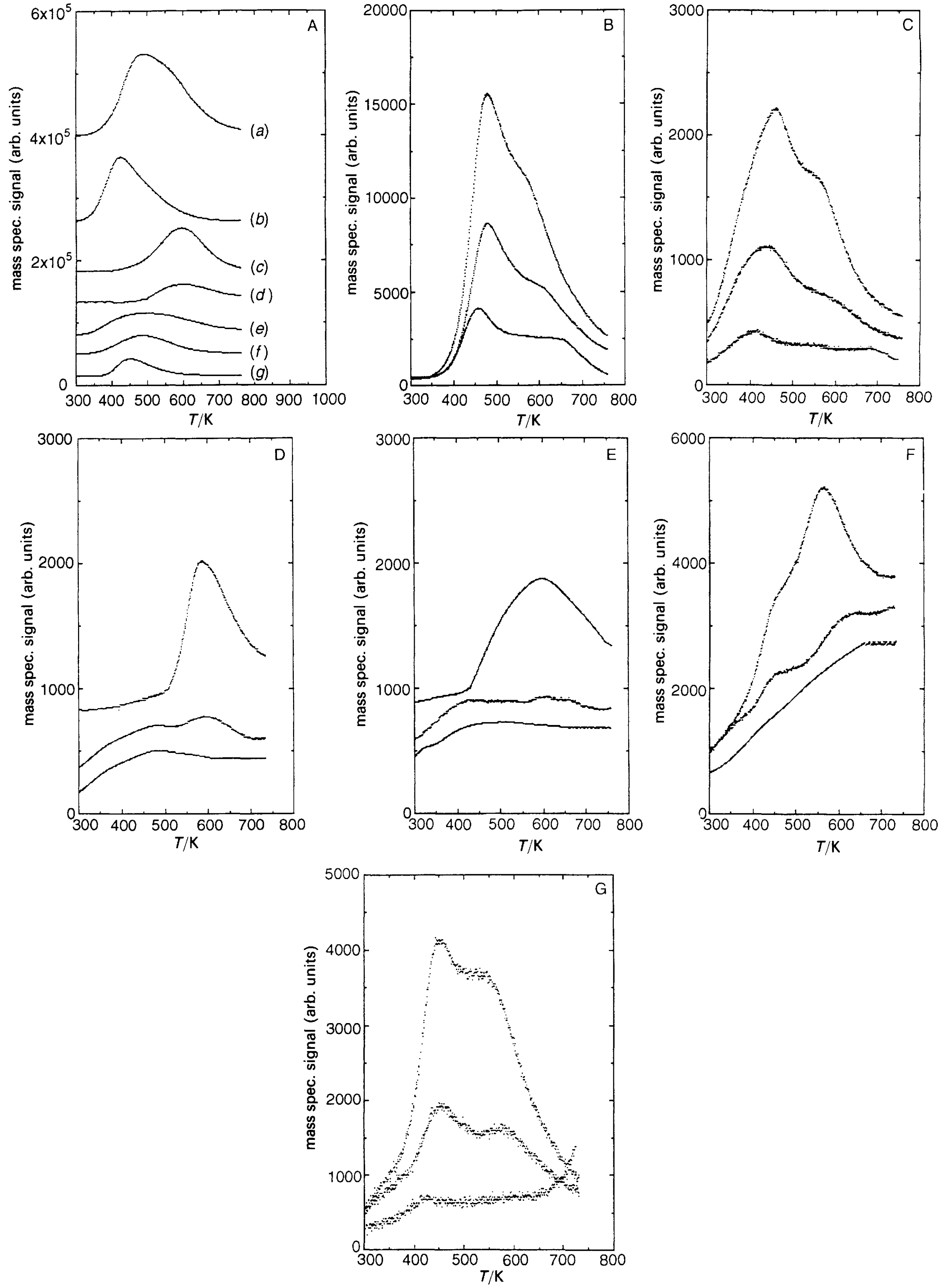

**Fig. 2** A, Thermal desorption spectra showing the product distribution from 3.0 Torr s of methanol adsorbed on $TiO_2$ at room temperature: (*a*) $CH_4$, (*b*) $CH_3OH$, (*c*) CO, (*d*) $H_2$, (*e*) $H_2O$, (*f*) HCHO, (*g*) DME. B, Thermal desorption spectra showing the evolution of $CH_4$ after dosing methanol onto $TiO_2$ at room temperature. The doses are 0.12, 0.24 and 0.5 Torr s (scale × 5). C, Thermal desorption spectra showing the evolution of $CH_3OH$ after dosing methanol onto $TiO_2$ at room temperature. The doses are 0.12, 0.24 and 0.5 Torr s (scale × 4). D, Thermal desorption spectra showing the evolution of CO after dosing methanol onto $TiO_2$ at room temperature. The doses are 0.12, 0.24 and 0.5 Torr s (scale × 1). E, Thermal desorption spectra showing the evolution of $H_2$ after dosing methanol onto $TiO_2$ at room temperature. The doses are 0.12, 0.24 and 0.5 Torr s (scale × 1). F, Thermal desorption spectra showing the evolution of $H_2O$ after dosing methanol onto $TiO_2$ at room temperature. The doses are 0.12, 0.24 and 0.5 Torr s (scale × 6.7). G, Thermal desorption spectra showing the evolution of HCHO after dosing methanol onto $TiO_2$ at room temperature. The doses are 0.12, 0.24 and 0.5 Torr s (scale × 20).

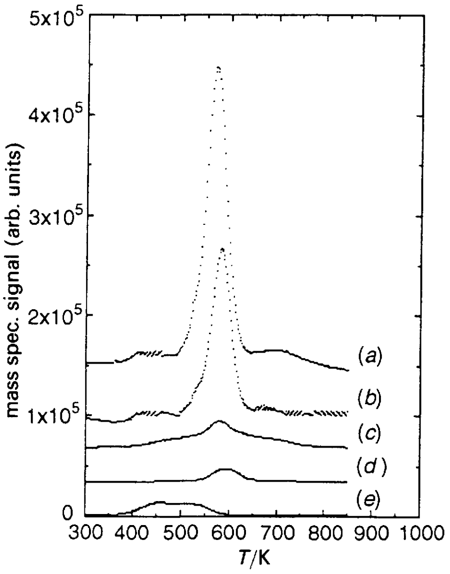

**Fig. 3** Thermal desorption spectra showing the product distribution from 0.15 Torr s of methanol adsorbed on SrO at room temperature: (*a*) $H_2$, (*b*) CO, (*c*) $H_2O$, (*d*) $CO_2$, (*e*) $CH_3OH$

the desorption is shifted much higher in temperature to 620 K. Following the second exposure, all the other species have also appeared and with the exception of $CH_4$, these are predominantly evolved in the lower-temperature state. At saturation, the $CH_3OH$ peak has broadened and is shifted by 10 K to lower temperatures.

When this oxide was heated in oxygen in the same way as $TiO_2$, the result was again to decrease the evolution of $CH_4$ and increase that of $H_2O$.

## Discussion

### Surface Characterisation by XPS

The XPS results have shown that it is difficult to prepare SrO in a pure form. Mohri *et al.*[8] indicated that heat treatment above 873 K was necessary to observe any catalytic activity of SrO for the isomerisation of but-1-ene. They prepared SrO from $Sr(OH)_2$ and attributed the lack of activity at lower pretreatment temperatures to the presence of $CO_2$ on the surface which blocked the reaction. When the oxide was heated by itself, they observed the evolution of $H_2O$ at 623 K and $CO_2$ at 973 K. Heating to higher temperatures did not increase the amount of $CO_2$ evolved which was estimated to be 40 times as much as would be needed to make a monolayer on the oxide surface. Coluccia and Tenck[11] found that heating the sample at 953 K led to the complete bulk decomposition of $SrCO_3$ to SrO, although they could still detect some $CO_2$ on the surface with IR.

In the present case, SrO had to be transported through air for the XPS analysis which will have led to $CO_2$ and $H_2O$ uptake. The carbonate and hydroxide thus formed which dominate the spectrum could not be decomposed properly as the sample heating on this instrument was limited to around 770 K. Consequently, a spectrum of pure SrO could not be obtained. As far as the surface stoichiometry of SrO is concerned no conclusions can therefore be drawn. (SrO has a rocksalt structure. It is cubic face-centred and each Sr atom is surrounded by six O atoms and *vice versa*.) However, it is assumed that the oxide surface was predominantly composed of oxide during the thermal desorption experiments as it had been heated to 973 K before these were carried out.

As was pointed out in the Results section, the binding energy values of Ti 2p and O 1s in $TiO_2$ are identical to those in $SrTiO_3$. As far as the O 1s position is concerned, no simple correlation between the binding energy and the metal oxide bond character in general has been found so far.[31] For Ti it is concluded that it is in the same oxidation state in both oxides. In ref. 27 and 28 it was stated that it is very difficult to reduce either oxide by heating *in vacuo* or even heating in $H_2$ at the temperatures employed here. Only after argon-ion bombardment was it possible to observe $Ti^{3+}$. The results presented here are consistent with this statement. Only $Ti^{4+}$ is detected and the atomic ratio Ti : O indicates a stoichiometric $TiO_2$ surface. The $TiO_2$ surface is often considered to be best represented by the (110) plane, as its preparation by cleavage *in vacuo* requires the breakage of the fewest number of bonds. It is visualised as consisting of bridging oxygen atoms in the [001] direction on top of every second row of in-plane Ti atoms. This ensures that half the Ti atoms have six-coordination and half have five-coordination.[32,33]

For $SrTiO_3$, two model surfaces have been proposed by Heinrich.[33] The (111) surface consists of a layer of SrO on which Ti atoms are located in three-fold oxygen sites. The (100) surface is composed of alternating layers of SrO and $TiO_2$ and the crystal termination is either the one or the other or a mixture of both. A recent STM study of this surface suggested that it always has a $TiO_2$ face which consists of a (2 × 2) ordered oxygen vacancy structure with Sr scattered on top.[34]

In the work presented here, $SrTiO_3$ was found to be depleted in Ti and enriched in Sr and O at the surface. This is contrary to the observations of Lo and Somorjai who were interested in compositional changes of an $SrTiO_3(111)$ surface following different treatments.[19] They established that heating the stoichiometric surface at 873 K *in vacuo* resulted in a decrease in both the Sr : O and Ti : O ratios. This change was found to be a reversible process as the original values were restored by cooling the sample to room temperature. Sputtering led to the preferential removal of O and Ti, and subsequent heating caused diffusion of Sr into the bulk. In contrast to this, high-temperature sputtering produced an Sr-rich surface. As far as the $SrTiO_3$ powder is concerned, it must be assumed that these models are useful as a first approach to understanding the surface structure of the two oxides, but that they are too simplified to account for all the observations. The exposure of a range of different planes as the surface as well as the presence of defects will influence the results, and these factors have not been considered in the models.

Lastly, the XPS results revealed that the surfaces of the oxides are hydroxylated. In the Introduction, it was already quoted that Ferrer and Somorjai[16] found the surface of $SrTiO_3(111)$ to contain residual hydroxy groups after it had been cleaned and heated *in vacuo*. $TiO_2$ is well known to dehydroxylate on heating *in vacuo*.[35] The greatest loss of OH takes place up to 600 K after which a slow further decrease in the number of hydroxy groups with time and temperature is obtained, although it never reaches zero. This is consistent with the results presented here. It is interesting to note that although $SrTiO_3$ underwent the same heat treatment as $TiO_2$ its surface remains more hydroxylated.

### Thermal Desorption Experiments

The mechanism of methanol adsorption and decomposition is generally explained in the following way.[36,37] The initial adsorption of methanol can be either molecular [step (1)] or dissociative [step (2)]:

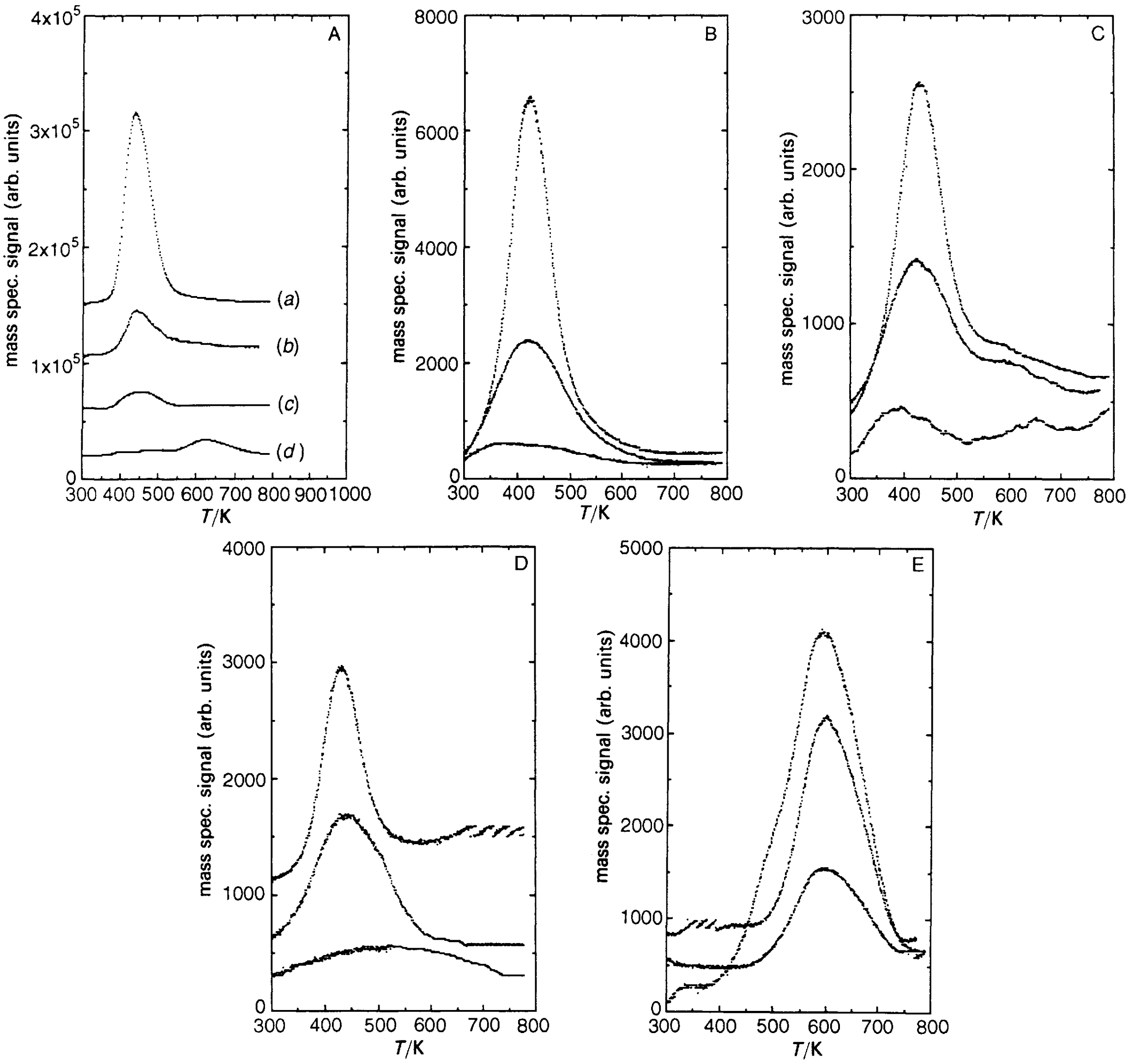

**Fig. 4** A, Thermal desorption spectra showing the product distribution from 3.0 Torr s of methanol adsorbed on $SrTiO_3$ at room temperature; (*a*) $CH_3OH$, (*b*) $H_2$, (*c*) $H_2O$, (*d*) $CH_4$. B, Thermal desorption spectra showing the evolution of $CH_3OH$ after dosing methanol onto $SrTiO_3$ at room temperature. The doses are 0.12, 0.24 and 0.5 Torr s (scale × 5). C, Thermal desorption spectra showing the evolution of $H_2$ after dosing methanol onto $SrTiO_3$ at room temperature. The doses are 0.12, 0.24 and 0.5 Torr s (scale × 1). D, Thermal desorption spectra showing the evolution of $H_2O$ after dosing methanol onto $SrTiO_3$ at room temperature. The doses are 0.12, 0.24 and 0.5 Torr s (scale × 6.7). E, Thermal desorption spectra showing the evolution of $CH_4$ after dosing methanol onto $SrTiO_3$ at room temperature. The doses are 0.12, 0.24 and 0.5 Torr s (scale × 5).

$$CH_3OH_g \rightarrow CH_3OH_a \qquad (1)$$

$$CH_3OH_a \rightarrow CH_3O_a + H_a \qquad (2)$$

The dissociative adsorption is thought to occur at a coordinatively unsaturated Ti cation ($Ti_v$) and an oxygen anion [step (3)]:

$$CH_3OH_g + O_s + Ti_v \rightarrow CH_3O_a + OH_a \qquad (3)$$

The methoxy species thus formed can react in several ways, one of which is by recombining [the reverse of step (2)] to form methanol. This would lead to molecular desorption. Alternatively, the methoxy group can dehydrogenate further to yield HCHO and $H_2$ in the vacuum [steps (4)–(6)]:

$$CH_3O_a \rightarrow CH_2O_a + H_a \qquad (4)$$

$$CH_2O_a \rightarrow CH_2O_g \qquad (5)$$

$$CH_2O_a \rightarrow CO_g + H_{2g} \qquad (6)$$

In fact, the coincident desorption of $CH_3OH$, HCHO and $H_2$ has been taken as proof of the existence of methoxy groups on a ZnO surface.[36] If the surface is in a reduced state and hence binds the oxygen in methoxy strongly a further reaction is possible. In order to replace this oxygen vacancy on the surface the C—O bond may be broken and the oxygen atom incorporated as surface lattice oxygen, $O_s$ [step (7)]:

$$CH_3O_a \rightarrow CH_{3a} + O_s \qquad (7)$$

This frees the methyl group which can react with adsorbed H or OH from step (3) to be released as $CH_4$ [step (8)] or it can decompose further to adsorbed C and H [step (9)].

$$CH_{3a} + H_a \rightarrow CH_{4g} \qquad (8)$$

$$CH_{3a} \rightarrow C_a + 3H_a \qquad (9)$$

The removal of hydroxy groups or oxygen deposited in steps (3) and (7) can occur in two ways, either through disproportionation of neighbouring hydroxy groups [step (10)] or through the reaction of adsorbed H with adsorbed O and OH [step (11)].

$$OH_a + OH_a \rightarrow H_2O + O_a \qquad (10)$$

$$OH_a + H_a \rightarrow H_2O_g \qquad (11)$$

Kim pointed out that oxygen could also be removed through the oxidation of carbon deposited in step (9) [step (12)]:

$$C_a + O_a \rightarrow CO_g \qquad (12)$$

The evolution of $(CH_3)_2O$ has generally been explained as a bimolecular reaction which requires two neighbouring methoxy species [step (13)]:

$$CH_3O_a + CH_3O_a \rightarrow (CH_3)_2O_g + O_a \qquad (13)$$

On ZnO Bowker *et al.*[36] found that adsorbed methoxy groups could undergo a further reaction. Here they coexisted with formate on the surface, the former decomposing into $CH_3OH$, HCHO, $H_2$ and CO at 380 K while the latter decomposed into mainly CO and $H_2$ together with small amounts of $CO_2$ and $H_2O$ at 580 K. Methoxy groups are initially oxidised by basic centres on the surface, leading to the binding of the methoxy carbon to another oxygen atom with rapid deprotonation to leave formate [step (14)]. The formate decomposes according to steps (15) and (16).

$$CH_3O_a + 3O_s \rightarrow HCOO_a + 2OH_a \qquad (14)$$

$$HCOO_a \rightarrow CO_g + H_a + O_s \qquad (15)$$

$$H_a + H_a \rightarrow H_{2g} \qquad (16)$$

Kim *et al.*[24,37] observed on the (011) facetted surface of single-crystal $TiO_2(001)$ and $TiO_2$ powder (both anatase) that molecularly adsorbed $CH_3OH$ was desorbed predominantly at 275 K and was completely removed at 365 K. Onishi *et al.*,[25] using UPS, also found methanol to be adsorbed molecularly on $TiO_2(110)$ and (441). In the work presented here, it is not possible to decide whether methanol is adsorbed molecularly [step (1)] or dissociatively [step (2)]. In any case, the dissociation according to steps (2) and (3) occurs once the thermal desorption experiment is started, as a range of decomposition products are observed which are attributed to the adsorbed intermediate methoxy groups. Different decomposition paths are in competition with each other and their relative probability will depend on the temperature, the coverage, the state of the adsorption site and the availability of other species like H and O. At low coverage, $CH_4$ formation is favoured. This must imply that the surface is in a partially reduced state containing coordinatively unsaturated centres and vacancies. On the one hand, the XPS results indicated that the original surface is stoichiometric and consists of $Ti^{4+}$ only. On the other hand, the oxidation experiment described in the Results section showed that the $TiO_2$ surface is reduced during the thermal desorption of methanol. The introduction of vacancies must therefore be attributed to preliminary desorption experiments which were carried out. This would leave the surface in a partially reduced state made up of both $Ti^{3+}$ and O lattice vacancies. These then have a reduced coordination and will react to restore saturation. The adsorption of methanol hence takes place according to step (3) and the filling of the O vacancy is complete once the C—O bond of the methoxy group is broken [step (7)]. This becomes an irreversible process as far as methanol is concerned and results in $CH_4$ formation [step (8)]. In this way, through every decomposed molecule of $CH_3OH$ the surface gains one atom of oxygen. If this was a continuous process it would be expected that the adsorption behaviour would change from that of a reduced surface to that of an oxidised surface with increasing exposure. In that case, the evolution of $CH_4$ would be expected to decrease with the number of lattice oxygen vacancies. As this is not the case here, it must be inferred that the oxygen that is deposited in step (7) does not remain on the surface but is removed during the TPD experiment. The evolution of $H_2O$ takes place over a wide temperature range and is most likely to account for the loss of O from the surface [steps (10) and (11)]. In fact, it might be speculated that the first loss of $H_2O$ initiates further decomposition of adsorbed methanol through the creation of further vacancies. After the thermal desorption, the surface is essentially unchanged, that is, it is in the same state as before the adsorption of methanol. It is worth noting that Kim *et al.* also found the oxide to be reduced during use and that they detected $H_2O$ desorption over the temperature range 350–600 K during thermal desorption of methanol from $TiO_2$ anatase.[24,37]

At higher methanol exposures, the reversible adsorption becomes more probable [reversal of step (2)]. The higher concentration of methanol and methoxy groups on the surface means that the existing vacancies can be filled and that at the same time other reaction paths are available. This is seen in the increased evolutions of $CH_3OH$, HCHO, $H_2$ and CO. $CH_4$ formation still occurs and it takes place at two different temperatures. This is indicative of two different sites on the surface which participate in this reaction. These two sites also give rise to methanol and HCHO, the former being formed through the reversal of steps (2) and (3), while the latter is formed according to steps (4) and (5). The H liberated through step (4) is not desorbed [step (6)] but instead is consumed in the reformation of methanol [reversal of steps (2) and (3)] or alternatively remains on the surface as OH. From Fig. 2A it is seen that the formation of $CH_4$ is more favourable at 440 K than at 580 K while CO and $H_2$ are evolved only at the higher temperature. The coincident evolution of CO and $H_2$ is attributed to the further oxidation of HCHO formed from methoxy [steps (4)–(6)] which is likely to proceed *via* a formate intermediate. The fact that $H_2$ is of lower intensity than CO is due to its consumption in the production of $H_2O$ [step (11)] and $CH_4$ [step (8)].

Kim *et al.*[37] observed the evolution of CO which they attributed to the oxidation of carbon deposits at temperatures in excess of 600 K. In the present work CO evolution took place at slightly lower temperatures and it was accompanied by $H_2$ evolution. This indicates that it is linked to the decomposition of methoxy groups rather than being a result of carbon oxidation. Repeated adsorption experiments also did not reveal any major decrease in activity, so a blockage of the surface by carbon had not occurred. It is concluded that steps (9) and (12) do not take place here.

The evolution of $(CH_3)_2O$ according to step (13) is only feasible if two methoxy species are adsorbed next to each other. It is therefore not surprising that this product is only evolved following the highest exposure and that it is desorbed before other reactions become dominant and remove methoxy. Similarly, Fig. 2A shows that following the highest exposure the $CH_3OH$ desorption peaks at low temperatures and is lost before other reactions like the formation of $CH_4$ became dominant.

These results are in qualitative agreement with those of Suda *et al.*[38] and Ramis *et al.*[39] who using IR found that methanol and other alcohols were adsorbed dissociatively to form alkoxides on $TiO_2$ (rutile) which they attributed to the dehydroxylated state of the surface. Cunningham *et al.*,[40] who also studied alcohol adsorption on $TiO_2$ (rutile) following extensive heating *in vacuo*, also observed the evolution of $CH_4$ together with some higher alkenes.

The work presented here also indicates that the adsorbed surface species on $TiO_2$ is the methoxy group. This contrasts strongly with the behaviour of methanol on SrO where the dominant desorptions are those of coincident CO and $H_2$ at 580 K. This pattern has been attributed to the existence of formate on the surface of ZnO as outlined above [steps (14)–(16)]. Both the temperature of desorption and the intensity of the products are very similar to the results obtained on ZnO.[36] The reversible adsorption of $CH_3OH$ also takes place but it is more limited than on $TiO_2$. On this oxide only one type of site is present which leads to one adsorbed species and one set of decomposition peaks. Formate was not detected on $TiO_2$ (anatase) or $TiO_2(00)$ by Kim *et al.*[24,37]

On $SrTiO_3$, there are again two types of sites available as indicated by the two desorption states. However, the thermal desorption of adsorbed methanol differs from that on both the other oxides. As was shown with XPS this surface is more highly hydroxylated and possibly enriched in O and Sr/depleted in Ti. Both these factors would decrease the likelihood of forming $CH_4$. This is indeed confirmed by the fact that $CH_4$ is only evolved in the higher-temperature state. This $CH_4$ evolution is qualitatively similar to that from $TiO_2$ in that it is affected by the oxidation of the surface, but it is shifted to significantly higher temperatures and it is of lower intensity. It may correspond with the high-temperature peak seen in the low-coverage data from $TiO_2$. The increased abundance of oxygen on this surface has successfully blocked the low-temperature route to $CH_4$ in favour of $CH_3OH$ desorption. Methoxy groups are the likely intermediate to form $CH_4$, since coincident, minor products of CO and formaldehyde are seen. Methane formation presumably occurs by CO bond dissociation to fill what was previously an anion vacancy. A significant difference between this material and $TiO_2$ itself is the lack of CO evolution (compare Fig. 2 and 4), indicating no formate formation. This perhaps relates to the greater stability of the methoxy on the mixed oxide which in turn also alters the selectivity pattern.

These results are in agreement with the trend observed by others that a more reduced surface would tend to bind the oxygen of methanol strongly hence leading to dissociative adsorption followed by other reactions. In order for dissociation to take place a pair like $Ti^{3+}$ next to an oxygen vacancy is required which forms the reactive centre. On a more oxidised surface such a centre is less likely to exist. The adsorption therefore occurs on a single site and is more likely to be molecular. In this respect, although Kim *et al.* showed methanol to dissociate on a well oxidised $TiO_2(001)$ surface[24] (they detected methoxy groups by XPS after room-temperature adsorption), the most likely reaction during thermal desorption was the recombination to form $CH_3OH$ in the gas phase since reactive centres (vacancies) for further decomposition were not available. With respect to the results shown here, this is similar to the behaviour of methanol on $SrTiO_3$. The fact that two reaction sites are present on $SrTiO_3$ as well as on $TiO_2$ must be attributed to similar surface structures. The basic building block of both oxides is the $TiO_6$ octahedron. The inclusion of Sr cubes around these octahedra modifies the behaviour of $TiO_2$. The presence of Sr has influenced $TiO_2$ structurally and electronically, making it more difficult to remove surface hydroxy groups and shifting the high-temperature decomposition of methoxy groups to even higher temperatures. Although XPS results show an enrichment of Sr and O on $SrTiO_3$ this does not indicate the presence of an extended SrO structure, evidenced by the lack of formate formation and decomposition on $SrTiO_3$. This is attributed to the very much changed environment of Sr in $SrTiO_3$ as compared with Sr in SrO. From this point of view, an STM study of $SrTiO_3(100)$ found the surface structure to be dominated by an ordered oxygen/Ti structure, and this is reflected well in the surface behaviour of $SrTiO_3$ powder.[34]

The authors thank the SERC for the funding of the postdoctoral position to N.A. *via* the IRC in Surface Science.

## References

1 G. C. Bond, *Heterogeneous Catalysis: Principles and Applications*, Clarendon Press, Oxford, 1974, ch. 4, pp. 57–65.
2 H. H. Kung, *Transition Metal Oxides: Surface Chemistry and Catalysis*, (*Stud. Surf. Sci. Catal. 45*), Elsevier, Amsterdam, 1989, ch. 1, pp. 1–5.
3 S. J. Tauster, S. C. Fung and R. L. Garten, *J. Am. Chem. Soc.*, 1978, **100**, 170.
4 G. L. Haller and D. E. Resasco, *Adv. Catal.*, 1989, **36**, 173.
5 R. I. Bickley, *Specialist Periodical Report: Catalysis*, The Royal Society of Chemistry, London, 1982, pp. 309–332.
6 F. T. Wagner and G. A. Somorjai, *J. Am. Chem. Soc.*, 1980, **102**, 5494.
7 K. Domen, A. Kido, T. Onishi, N. Kosugi and H. Kuroda, *J. Phys. Chem.*, 1986, **90**, 292.
8 M. Mohri, K. Tanabe and H. Hattori, *J. Catal.*, 1974, **32**, 144.
9 G. Zhang, H. Hattori and K. Tanabe, *Appl. Catal.*, 1988, **36**, 189.
10 K. Tanabe, *Catalysis Science and Technology*, ed. J. R. Anderson and M. Boudart, Springer-Verlag, Berlin, 1981, vol. 2, pp. 231–273.
11 S. Coluccia and A. J. Tenck, *J. Chem. Soc., Faraday Trans. 1*, 1983, **79**, 1881.
12 M. T. Xu and J. H. Lunsford, *Catal. Lett.*, 1991, **11**, 295.
13 S. J. Conway, J. A. Greig and G. M. Thomas, *Appl. Catal. A*, 1992, **86**, 199.
14 M. I. Sosulnikov and Yu A. Teterin, *J. Electron Spectrosc. Relat. Phenom.*, 1992, **59**, 111.
15 *Gmelins Handbuch der Anorganischen Chemie*, System-Nr. 41, 8. Auflage, Verlag Chemic, Weinheim, 1951, p. 433.
16 S. Ferrer and G. A. Somorjai, *Surf. Sci.*, 1980, **94**, 41.
17 S. Ferrer and G. A. Somorjai, *Surf. Sci.*, 1980, **97**, L304.
18 R. G. Egdell and P. D. Naylor, *Chem. Phys. Lett.*, 1982, **91**, 200.
19 W. J. Lo and G. A. Somorjai, *Phys. Rev. B*, 1978, **17**, 4942.
20 W. J. Lo, Y. W. Chung and G. A. Somorjai, *Surf. Sci.*, 1978, **71**, 199.
21 V. E. Heinrich, G. Dresselhaus and H. J. Zeiger, *Solid State Commun.*, 1977, **24**, 623.
22 W. Gopel, G. Rocker and R. Feierabend, *Phys. Rev. B*, 1983, **28**, 3427.
23 C. A. Muryn, P. J. Hardman, J. J. Crouch, G. N. Raiker, G. Thornton and D. S-L. Law, *Surf. Sci.*, 1991, **251/252**, 747.
24 K. S. Kim and M. A. Barteau, *Surf. Sci.*, 1989, **223**, 13.
25 H. Onishi, T. Aruga, C. Egawa and Y. Iwasawa, *Surf. Sci.*, 1988, **193**, 33.
26 E. Roman and J. L. de Segovia, *Surf. Sci.*, 1991, **251/252**, 742.
27 A. F. Carley, P. R. Chalker, J. R. Riviere and M. W. Roberts, *J. Chem. Soc., Faraday Trans. 1*, 1987, **83**, 351.
28 C. N. Sayers and N. R. Armstrong, *Surf. Sci.*, 1978, **77**, 301.
29 D. R. Penn, *J. Electron Spectrosc. Relat. Phenom.*, 1976, **9**, 29.
30 J. H. Scofield, *J. Electron Spectrosc. Relat. Phenom.*, 1976, **8**, 129.
31 N. S. McIntyre, in *Practical Surface Analysis by Auger and X-Ray Photoelectron Spectroscopy*, ed. D. Briggs and M. P. Seah, John Wiley, Chichester, 1983, ch. 10, p. 410.
32 G. S. Rohrer, V. E. Heinrich and D. A. Bonnell, *Surf. Sci.*, 1992, **278**, 146.
33 V. E. Heinrich, *Prog. Surf. Sci.*, 1983, **14**, 175.
34 T. Matsumoto, H. Tanaka, T. Kawai and S. Kawai, *Surf. Sci.*, 1992, **278**, L153.
35 A. H. Boonstra and C. A. H. A. Mutsaers, *J. Phys. Chem.*, **1975**, **79**, 1694.
36 M. Bowker, H. Houghton and K. C. Waugh, *J. Chem. Soc., Faraday Trans. 1*, 1981, **77**, 3023.
37 K. S. Kim, M. A. Barteau and W. F. Farneth, *Langmuir*, 1988, **4**, 533.
38 Y. Suda, T. Morimoto and M. Nagao, *Langmuir*, 1987, **3**, 99.
39 G. Ramis, G. Busca and V. Lorenzelli, *J. Chem. Soc., Faraday Trans. 1*, 1987, **83**, 1591.
40 J. Cunningham, D. J. Morrissey and E. L. Goold, *J. Catal.*, 1978, **53**, 68.

*Paper* 3/06196E; *Received* 18*th October*, 1993